

# How Mantle Slabs Drive Plate Tectonics

Clinton P. Conrad\* and Carolina Lithgow-Bertelloni

The gravitational pull of subducted slabs is thought to drive the motions of Earth's tectonic plates, but the coupling between slabs and plates is not well established. If a slab is mechanically attached to a subducting plate, it can exert a direct pull on the plate. Alternatively, a detached slab may drive a plate by exciting flow in the mantle that exerts a shear traction on the base of the plate. From the geologic history of subduction, we estimated the relative importance of "pull" versus "suction" for the present-day plates. Observed plate motions are best predicted if slabs in the upper mantle are attached to plates and generate slab pull forces that account for about half of the total driving force on plates. Slabs in the lower mantle are supported by viscous mantle forces and drive plates through slab suction.

Although the motions of Earth's tectonic plates are generally accepted to be the surface expression of convection in Earth's mantle (1), the mechanism by which mantle convection drives plate motions has been the subject of debate for some time (2–7). Mantle convection may be driven primarily by the descent of dense slabs of subducted oceanic lithosphere (8–10), which are the most prominent density heterogeneities in the mantle (11, 12). The motions of the surface plates have also been attributed to the pull from descending slabs (2–7, 13), but it is not clear whether the two are directly coupled, or whether induced mantle flows transmit stresses from slabs to plates. If slabs remain mechanically attached to the surface plates as they subduct, then slabs can act as stress guides that transmit the downward pull of dense mantle slabs directly to plate boundaries (14). These "slab pull" forces drive subducting plates toward subduction zones. Alternatively, if slabs in the mantle are not well attached to the surface plates, then descending slabs may induce mantle circulation patterns that exert shear tractions at the base of nearby plates. These "slab suction" forces have been shown to cause both subducting and overriding plates to move toward subduction zones (1, 5–8, 15).

To determine the relative importance of the slab pull and slab suction forces for the mantle, we examined a model of present-day slab locations (6, 16, 17) that was computed from Cenozoic (18) and Mesozoic (6) plate reconstructions. Using the history of subduction since the Mesozoic, we defined the material in the slab location model that has been part of continuous

subduction for each of the nine most tectonically active present-day subduction zones (Fig. 1). The excess weight of this material should generate the slab pull force, but only if the slab remains mechanically coherent within the mantle. Rapid trench migration and the phase transition at 660 km may cause slab coherency to deteriorate (19). Thus, we estimated slab pull forces on the basis of the excess weight of all connected slab material, subject to an inclusion

criterion that corresponds to a maximum allowable rate of trench migration at the surface (17). We defined three models for the slab pull force that used rollback rate cutoffs of 10% or 25% (20) and included or excluded material below 660 km (Fig. 1). Slab pull is applied normal to subducting plate boundaries and totals  $1.9 \times 10^{21}$  N for all upper-mantle slabs. By comparison, slab suction shear tractions from both upper- and lower-mantle slabs total  $1.6 \times 10^{21}$  N. Thus, the slab pull force can be comparable to, or even more important than, the slab suction force as a plate-driving mechanism.

Because the slab pull and slab suction plate driving mechanisms act differently on subducting and overriding plates, they should generate different patterns of surface plate motion. To constrain the relative importance of these mechanisms, we compared observed plate motions (17) with predicted plate motions that we computed from the slab pull and slab suction driving mechanisms (Fig. 2). We predicted plate velocities by first computing resisting shear tractions that are induced by viscous flow in the mantle (6, 15) and then enforcing the no-net-torque approximation for each plate (2). The predicted plate velocity field depends on the mantle viscosity structure,

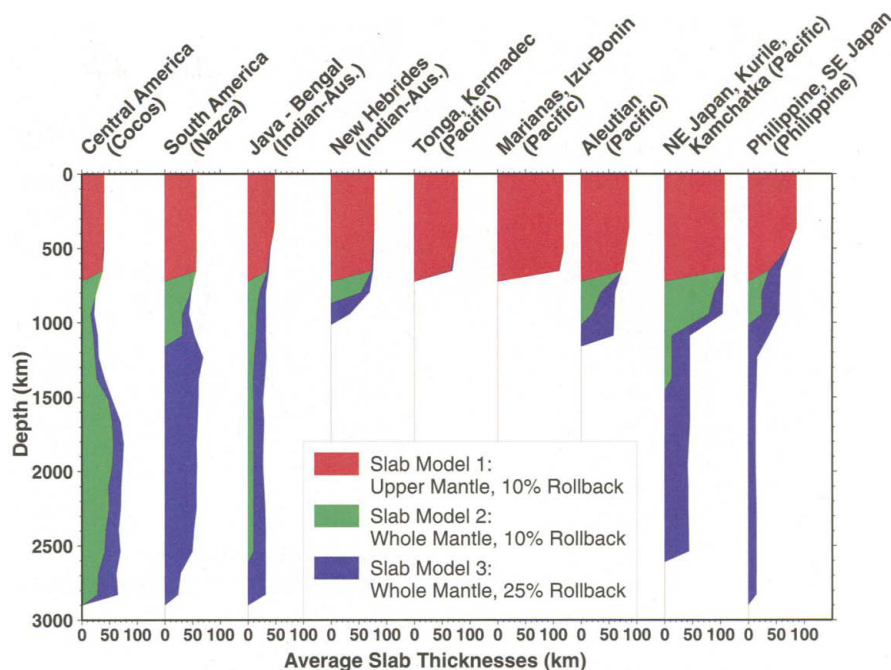


**Fig. 1.** Profiles of the slab material attached to the nine subduction zones used in this study. Slab thickness is expressed as  $2(\kappa t_c)^{1/2}$ , where  $t_c$  is the average age of the slab at the time of subduction and  $\kappa = 10^{-6} \text{ m}^2 \text{ s}^{-1}$  is the thermal diffusivity. Although average slab thicknesses are shown here, variations in thickness along the length of each slab are important and are included in the determination of the pull forces on plates. In slab model 1 (red), slab material is restricted to the upper mantle. In slab models 2 and 3, slab material is permitted in the lower mantle but restricted to a departure from verticality represented by 10% trench rollback (model 2, green) or 25% trench rollback (model 3, blue). The plate to which each slab is attached is shown in parentheses. The total excess mass of attached slabs is  $1.3 \times 10^{20}$ ,  $2.9 \times 10^{20}$ , and  $7.0 \times 10^{20}$  kg for models 1, 2, and 3, respectively.

Department of Geological Sciences, University of Michigan, Ann Arbor, MI 48109, USA.

\*To whom correspondence should be addressed. E-mail: cpconrad@umich.edu

## REPORTS

which we take to be the one that gives the best fit to the geoid for the slab heterogeneity model (6). Our calculations did not include any possible lateral variations in viscosity, which can affect the relative coupling of continental and oceanic plates to mantle flow (21). This simplification should have a greater effect on patterns of plate motions driven by slab suction than on those of plate motions driven by slab pull, because the former plate-driving mechanism depends directly on plate-mantle coupling while the latter does not.

If the driving torques on plates are generated by the slab suction mechanism acting alone, the predicted plate velocity field (Fig. 2A) differs from the observed plate velocity field (17) (Fig. 2B) in several ways. Most important, the slab suction model causes overriding plates to move toward neighboring subduction zones at speeds comparable to those of the subducting plates (Fig. 2A); this differs from the basic observa-

tion that plates with subduction zones move at 3 to 4 times the rate of plates without subduction zones (18, 22). This difference in plate speeds, which has been the subject of both controversy and study (18, 21), cannot be produced by the slab suction mechanism acting alone, because the pattern of mantle flow excited by downgoing slabs exerts shear tractions equally (symmetrically) on both subducting and overriding plates. In addition, the slab suction mechanism causes subducting plates such as the Pacific, and the smaller Cocos and Nazca plates in particular, to move too slowly relative to the others—and, in the case of the Nazca plate, in the wrong direction.

Slab pull forces acting by themselves also cause subducting plates to move toward subduction zones (Fig. 2C), but in this case they move more quickly than the overriding plates. The pattern of plate speeds (Fig. 2C) is similar to that of the observed plate motions (Fig. 2B), with both showing a ring of slowly

moving overriding plates that surround the faster subducting plates in the Pacific basin. The most important discrepancy between the predicted and observed fields is that the slab pull mechanism causes overriding plates to move slowly away from subduction zones (Eurasia, North America, and South America in Fig. 2C), whereas these plates move slowly toward subduction zones in the observed field (Fig. 2B). This motion in the wrong direction occurs because the mantle flow pattern generated by the motion of subducting plates toward subduction zones typically causes overriding plates to move in the same direction as subducting plates. This counterintuitive asymmetrical effect of the slab pull mechanism is the key to understanding the difference between the observed speeds of subducting and overriding plates.

Compared to observed plate motions, overriding plates in the slab suction model move too rapidly in the right direction (toward subduction

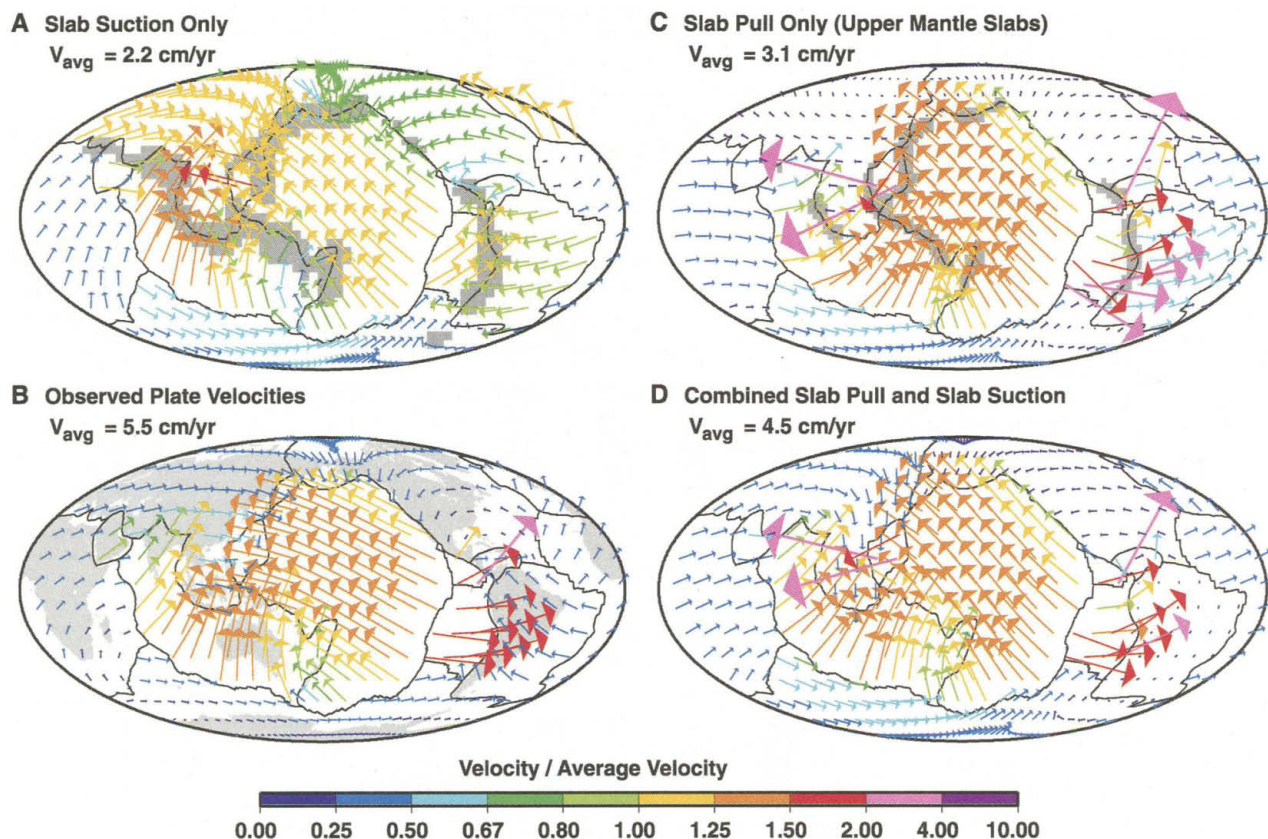


**Fig. 2.** A comparison of plate velocity fields, all shown in the no-rotation frame of reference. In all models, plate velocities are shown as arrows whose length is proportional to and whose color corresponds to the magnitude of velocity relative to the average plate velocity. (A) Results from the slab suction model, in which mantle slabs drive plates by inducing a mantle circulation that exerts shear tractions at the base of plates (6). The location of slabs at 660 km is shown in gray for comparison. In this model, overriding plates move nearly as fast as subducting plates. This deviates from the velocity field of observed plate motions, shown in (B), in which overriding plates move at one-fourth to one-third the rate of subducting plates, as demonstrated by the blue ring

of plate velocities surrounding the red- and orange-colored velocities of the Pacific, Nazca, Cocos, and Indian-Australian plates. Continental locations are shown in gray for reference. Overriding plates typically move with the correct speed, but in the wrong direction, if (C) plate velocities are calculated from slab pull forces alone; in this case the pull from attached upper-mantle slabs (slab model 1) is applied to subducting plates and forces from unattached slabs are ignored. If the pull force from attached upper-mantle slabs operates along with the suction force from unattached lower-mantle slabs, as in (D), the plate velocity field more closely matches the observed field for both the direction and the relative speeds of subducting and overriding plates.

zones), while overriding plates in the slab pull model move at the right speed but in the wrong direction (away from subduction zones). This suggests that a combination of the two models should cause both subducting and overriding plates to move in the correct direction at the correct speed. For simplicity, we calculate the plate velocities due to the combination of slab pull alone from upper-mantle slabs that are connected to surface plates (Fig. 1, slab model 1) and slab suction due to unconnected slabs (all slab material not in slab model 1). A comparison of this combined model (Fig. 2D) with the observed plate motions (Fig. 2B) shows that overriding plates now move in the correct direction and with about the right speed relative to the subducting plates. Indeed, with the exception of the South American plate, the motions of all the large subducting and overriding plates are well reproduced. The direction and speed of several smaller plates, particularly the Cocos and Nazca plates, are improved relative to the slab suction model alone. One exception is the Philippine plate, which moves faster in the combined model than is observed. Because it is surrounded by subduction zones, the Philippine plate's motion is poorly constrained, as exemplified by the large variation in published velocities for this plate, which range from more than 8 cm/year (22) to less than 4 cm/year (18).

Depending on mantle viscosity, a portion of the excess weight of connected slab material may be dynamically supported by viscous stresses from the surrounding mantle. In this case, a slab would not exert a direct pull force on attached surface plates, but instead its weight would push the surrounding mantle downward, generating mantle flow and exciting the slab suction mechanism. To examine the possibility that connected slabs might be partially supported by local viscous stresses rather than by the slab itself through a stress guide to the surface plates, we examined models in which the excess mass of connected slab material is partitioned between the slab pull and slab suction models by an adjustable amount (fig. S1). We found that the average speed of subducting plates relative to non-subducting plates increases as the slab pull mechanism becomes more important (fig. S1A). For the upper-mantle slab model, nearly the entire connected slab weight must serve as a pull force to obtain the observed velocity ratio of 3.6 (fig. S1A), and at least 70% must act as a pull force if the velocity ratio is 10% smaller than this. For the whole-mantle models, an even smaller fraction of the slab weight must be used (about 35% and 15% for slab models 2 and 3, respectively; fig. S1A). This is because the increased weight of these slabs requires a smaller fraction of their weight to act as pull in order to drive the subducting plates with a sufficient speed relative to

the overriding ones. The fraction of the pull force that produces an optimal ratio is approximately proportional to the relative total excess mass of the three slab models (Fig. 1). Thus, the total slab pull force corresponds to the pull from the entire excess weight of slabs in the upper mantle. If both upper- and lower-mantle slabs contribute to slab pull, then the total slab pull fraction must be reduced proportionally.

The slab pull forces from the three connected slab models produce different patterns of plate motions because the slabs in these models exhibit different pull forces relative to one another. Thus, the fit to observed plate motions should be different for different models, even when the total pull force is scaled to produce the correct ratio of subducting to nonsubducting plate velocities. We measured this fit with a normalized dot product between the observed plate velocity field and the field predicted by each model (17), a measurement that is sensitive to the relative directions of the two velocity fields. For the upper-mantle slab model, the direction of plate motions is fairly well predicted by both the slab suction and the combined models (7). As a result, the dot product is nearly constant between these two extremes for the upper-mantle model (fig. S1B). The dot product for the two whole-mantle models, however, is more than 20% below the value for the upper-mantle model (fig. S1B). Although these models do improve the ratio of subducting to overriding plate speeds, the directions and relative speeds of individual plates are poorly reproduced by the whole-mantle models compared to slab suction alone.

For the upper-mantle slabs, the model that yields the best prediction of the relative speeds of subducting and nonsubducting plates is one in which most of the excess weight of upper-mantle slabs participates in the pull force (fig. S1A). The net fit to the observed velocity field (fig. S1B) is nearly uniform between about 40% and 100% of upper-mantle slab weight causing slab pull, which corresponds to between 40 and 65% of the total force on plates (fig. S1C). If this pull force is distributed through the thickness of the subducting lithosphere, the lithosphere must act as a stress guide that is capable of supporting stresses between 200 and 500 MPa (17). The maximum value is close to laboratory estimates of the maximum shear stress that cold oceanic lithosphere can support (23), which suggests that the strength of slab material may limit the slab pull force. This maximum stress is larger than estimates of seismic stress drops, which are typically about 10 MPa, but seismicity may relieve only a fraction of the total background stress (24).

It is perhaps not surprising that lower-mantle material does not contribute to the

pull force on plates, because a factor of  $\geq 30$  increase in mantle viscosity is expected across the 660-km phase transition (10). This greater viscosity generates increased shear stresses on the sides of lower-mantle slabs, which tends to slow their descent but also tends to support them dynamically, decreasing their ability to contribute to the slab pull force. Moreover, the endothermic phase transition at 660 km may disrupt the descent of slabs and decrease their strength in the lower mantle (25). Both of these effects should disrupt the transmission of tensional stresses from lower-mantle slabs into the upper mantle. Our conclusion that the pull from lower-mantle slabs is not coupled to the surface plates also agrees with analyses of the effect of slabs on the observed geoid (26).

## References and Notes

1. D. L. Turcotte, E. R. Oxburgh, *J. Fluid Mech.* **28**, 29 (1967).
2. S. C. Solomon, N. H. Sleep, *J. Geophys. Res.* **79**, 2557 (1974).
3. D. Forsyth, S. Uyeda, *Geophys. J. R. Astron. Soc.* **43**, 163 (1975).
4. W. M. Chapelle, T. E. Tullis, *J. Geophys. Res.* **82**, 1967 (1977).
5. B. H. Hager, R. J. O'Connell, *J. Geophys. Res.* **86**, 4843 (1981).
6. C. Lithgow-Bertelloni, M. A. Richards, *Rev. Geophys.* **36**, 27 (1998).
7. T. W. Becker, R. J. O'Connell, *Geochim. Geophys. Geosyst.* **2**, 2001GC000171 (2001).
8. D. McKenzie, *Geophys. J. R. Astron. Soc.* **18**, 1 (1969).
9. F. Richter, D. McKenzie, *J. Geophys. Res.* **44**, 441 (1978).
10. B. H. Hager, *J. Geophys. Res.* **89**, 6003 (1984).
11. S. P. Grand, R. D. van der Hilst, S. Widiyantoro, *GSA Today* **7**, 1 (1997).
12. H. Bijwaard, W. Spakman, E. R. Engdahl, *J. Geophys. Res.* **103**, 30055 (1998).
13. C. P. Conrad, B. H. Hager, *J. Geophys. Res.* **104**, 17551 (1999).
14. W. M. Elsasser, in *The Application of Modern Physics to the Earth and Planetary Interiors*, S. K. Runcorn, Ed. (Wiley, New York, 1969), pp. 223–249.
15. Y. Ricard, C. Vigny, *J. Geophys. Res.* **94**, 17543 (1989).
16. Y. Ricard et al., *J. Geophys. Res.* **98**, 21895 (1993).
17. See supporting data on Science Online.
18. R. G. Gordon, D. M. Jurdy, *J. Geophys. Res.* **91**, 12389 (1986).
19. U. Christensen, *Phys. Earth Planet. Inter.* **127**, 25 (2001).
20. Trench rollback rates (1 to 2 cm/year) are 10 to 25% of subduction rates (6 to 10 cm/year) (27). The larger value (25%) is about equal to the maximum amount of trench rollback for which a vertically coherent slab is found in experiments (19).
21. S. Zhong, *J. Geophys. Res.* **106**, 703 (2001).
22. A. E. Gripp, R. G. Gordon, *Geophys. Res. Lett.* **17**, 1109 (1990).
23. D. L. Kohlstedt et al., *J. Geophys. Res.* **100**, 17587 (1995).
24. T. C. Hanks, *Pure Appl. Geophys.* **115**, 441 (1977).
25. E. Ito, H. Sato, *Nature* **351**, 140 (1991).
26. L. Moresi, M. Gurnis, *Earth Planet. Sci. Lett.* **138**, 15 (1996).
27. R. D. Jarrard, *Rev. Geophys.* **24**, 217 (1986).
28. Supported by a fellowship from the David and Lucile Packard Foundation (C.L.-B.). We thank two anonymous reviewers for comments.

## Supporting Online Material

www.sciencemag.org/cgi/content/full/298/5591/207/

DC1

Materials and Methods

Fig. S1

20 May 2002; accepted 3 September 2002